

# Photochemistry of doubly *N*-confused porphyrin bonded to non-conventional high oxidation state Ag(III) and Cu(III) ions

Fábio M. Engelmann<sup>a</sup>, Ildemar Mayer<sup>a</sup>, Koiti Araki<sup>a,\*</sup>, Henrique E. Toma<sup>a</sup>,  
Maurício S. Baptista<sup>a</sup>, Hiromitsu Maeda<sup>b</sup>, Atsuhiko Osuka<sup>b</sup>, Hiroyuki Furuta<sup>b,c</sup>

<sup>a</sup> Instituto de Química, Universidade de São Paulo, C. Postal 26077, CEP 05513–970, São Paulo (SP), Brazil

<sup>b</sup> Department of Chemistry, Graduate School of Science, Kyoto University, Kyoto 606-8502, Japan

<sup>c</sup> Department of Chemistry and Biochemistry, Graduate School of Engineering, Kyushu University, Fukuoka 812-8581, Japan

Received 12 September 2003; received in revised form 13 January 2004; accepted 19 January 2004

## Abstract

The photophysical properties of the free base, silver(III) and copper(III) doubly *N*-confused porphyrin complexes were examined. The free base species exhibits a low fluorescence quantum yield of  $9.1 \times 10^{-3}$ , which is completely suppressed in the M(III) complexes. However, high singlet oxygen quantum yields were found for the Ag(III) ( $\phi_{\Delta} = 0.92$ ) and Cu(III) ( $\phi_{\Delta} = 0.66$ ) complexes. These results were ascribed to the enhanced intersystem crossing rates, induced by heavy atom effect, rather than to a redox quenching involving the metal ions in unusually high oxidation state. The confused porphyrins are photochemically stable in oxygen-free solution but are bleached more or less rapidly by the photogenerated singlet oxygen, in the absence of other quenchers.

© 2004 Elsevier B.V. All rights reserved.

**Keywords:** Doubly *N*-confused porphyrin; Singlet oxygen; Energy transfer

## 1. Introduction

The properties of porphyrins and analogous macrocycles have been systematically studied given their prevalence in biological systems and their remarkable photophysical, catalytic and electrocatalytic properties. In 1994, the synthesis of the first true porphyrin isomer, the *N*-confused porphyrin, NCP, was reported simultaneously by Furuta et al. [1] and Latos-Grazynski and co-workers [2], starting the systematic studies on this new series of porphyrin analogues [3,4]. This isomer has one confused pyrrole ring, forms square-planar complexes with both divalent and trivalent metal ions such as Ni(II) [2,5–7], Pd(II) [8], Pt(II) [9], Cu(II) [10,11], Ag(III) [12], and Cu(III) [13] ions, and their chemistry, spectroscopy, electrochemistry and magnetism have been systematically studied [14–20]. More recently, the *cis*-doubly *N*-confused porphyrin, *cis*-N<sub>2</sub>CP, and their Ag(III) and Cu(III) metal complexes have been prepared and characterized [21–23]. Also, the total electronic energy (B3LYP level) and nucleus-independent chemical shifts (NICS, B3LYP/6-31G\*\* level) of 95 *N*-confused isomers in

all possible tautomeric forms have been determined by DFT analysis [24,25]. Interestingly, the aromaticity of the ring estimated from the NICS values seems to be the predominant driving force only in the case of porphyrins and NCPs, while steric factors were shown to be dominant in the case of the isomers with higher number of confused pyrrole rings. In fact, in the case of doubly *N*-confused porphyrins, only the *cis*-confused isomer (M-HN<sub>2</sub>CP), which is the most stable regioisomer according to DFT calculations, has been synthesized [26].<sup>1</sup> The coordinated M(III) ion is highly stabilized and can be reduced only at  $-0.9$  V (versus SHE), while the macrocyclic ring is oxidized around 1.4 V [27].

It is known that singlet oxygen is involved in natural photochemical and photobiological processes, as well as in the therapeutic action of Type II PDT drugs. Porphyrins and their analogues generally exhibit high absorptivity in the phototherapeutic window, as well as an excited triplet state with appropriate energy and lifetime for efficient energy transfer to triplet oxygen. Belair et al [28] compared the photophysical properties of *N*-confused tetraphenylporphyrin in two tautomeric forms (in dimethylacetamide and CH<sub>2</sub>Cl<sub>2</sub>) with those of analogous porphyrins and chlorophylls demon-

\* Corresponding author. Tel.: +55-11-3091-3887;

fax: +55-11-3815-5579.

E-mail address: [koiaraki@iq.usp.br](mailto:koiaraki@iq.usp.br) (K. Araki).

<sup>1</sup> *Trans*-N<sub>2</sub>CP, wherein two pyrrole rings at the opposite sites are confused, has recently been synthesized.

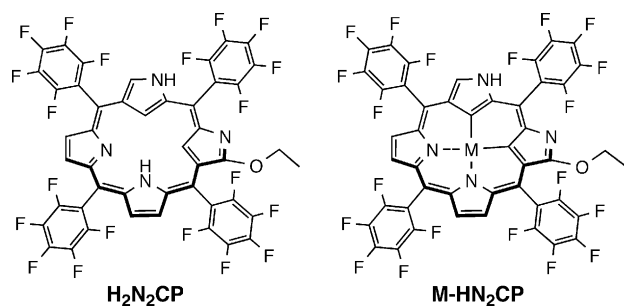


Fig. 1. Structures of the free base doubly *N*-confused porphyrin ( $H_2N_2CP$ ) and its metal complex ( $M-HN_2CP$ ).

strating the PDT potential of that isomer. Recently, we showed that the coordination of Ag(III) ion enhances about four times the efficiency of free base doubly *N*-confused porphyrin,  $H_2N_2CP$  (Fig. 1), as  $O_2(^1\Delta_g)$  sensitizer [29]. In this work, we report a detailed study on the photophysical properties of the free base  $H_2N_2CP$  and its Ag(III) and Cu(III) complexes ( $M-HN_2CP$ ), in order to improve the understanding of this new porphyrin type macrocycle.

## 2. Experimental

Doubly *N*-confused 2-ethoxy-5,10,15,20-tetrakis(pentafluorophenyl)-3,7-diaza-21,22-dicarbaporphyrin ( $H_2N_2CP$ ) and its silver ( $Ag^{III}HN_2CP$ ) and copper ( $Cu^{III}HN_2CP$ ) complexes were synthesized and characterized as previously described [21]. All solutions were prepared using spectroscopic grade acetonitrile from Aldrich. The protonated and deprotonated species were generated by bubbling a small amount of gaseous HCl or by adding tetrabutylammonium hydroxide (TBAOH), respectively, to the solution. This base was used instead of gaseous  $NH_3$  to avoid the possible suppression of the *cis*- $N_2CP$  excited state by that species.

The luminescence spectra were recorded on a Photon Technology Inc., model LS-100 spectrofluorimeter. The luminescence quantum yield measurements were carried out using a deaerated acetonitrile solution of meso-tetraphenylporphyrin (TPP) as standard ( $\phi_F = 0.15$ ). The triplet state lifetimes and excited state differential spectra were recorded using a time resolved absorption/emission spectrometer (Edinburgh Analytical Instruments LP900S1) equipped with a Nd:YAG laser (Spectron Laser System, UK) operating at 532 nm for sample excitation. The probing system was positioned at  $90^\circ$  and constituted by a 150 W pulsed Xenon lamp, a Czern-Turner monochromator and a germanium detector for the near infrared. The system was coupled with a Hewlett-Packard 54510B digital oscilloscope and a microcomputer for data acquisition. The experiments were carried out in the 300–700 nm range and the sample was refreshed before each series of experiments.

The singlet oxygen decay rates and the formation quantum yields were determined from the phosphorescence decay curves at 1270 nm. These data were recorded with a

time-resolved NIR fluorimeter (Edinburgh Analytical Instruments) equipped with a Nd:YAG laser (Continuum Surelite III) for sample excitation at 532 nm. The emitted light was passed through a silicon filter and a monochromator before being detected at a NIR-PMT (Hamamatsu Co. R5509). Methylene blue in air-saturated acetonitrile solution, at room temperature, was used as standard ( $\phi_\Delta = 0.50$ ). The curve fitting analysis of the Flash Photolysis and NIR emission decay curves was carried out using the Igor Pro 4.02 software (Wavemetrics). The sample solution was refreshed before each new series of experiments in order to minimize the interference of eventual photodecomposition byproducts.

1,3-Diphenylisobenzofuran (DPBF, 45  $\mu M$ ) was also used to determine the singlet oxygen quantum yields at room temperature, in air saturated acetonitrile solution. The samples were prepared immediately before use by transferring 10  $\mu l$  of the DPBF stock solution and 1 ml of a *cis*- $N_2CP$  acetonitrile solution ( $\sim 0.3$  a.u. at 480 nm) into a quartz cuvette in the dark. The experiments were carried out by irradiating the stirred sample with a 480 nm light beam provided by an Oriel Spectral Luminator (model 69070), while the absorbance at 411, 325 and 310 nm was simultaneously monitored using a diode array UV-Vis spectrophotometer (Agilent model 8453) in the kinetic mode. No significant changes were observed in the doubly confused porphyrin spectra above 500 nm during the experiments. The initial solution was used as reference in order to minimize errors.

A 150 W Xenon lamp light, filtered by passing through a 10 cm water layer and a UV filter (2 cm plexiglass plate) to remove the infrared and the UV radiation below 300 nm, was used in the photodecomposition experiments in deoxygenated acetonitrile solution. The samples (typically 20  $\mu M$ ) were carefully purged with nitrogen or argon gas and constantly stirred while measuring the UV-Vis spectra as a function of the time. A blanket of the corresponding inert gas was used during the experiments to minimize the possible contamination by oxygen. The experiments in oxygen-saturated solutions were carried out in the same way using  $O_2$  gas instead.

## 3. Results and discussion

In contrast to normal porphyrins, the doubly *N*-confused free base porphyrin ( $H_2N_2CP$ ) exhibits two confused adjacent pyrrole rings, providing two carbon and two nitrogen atoms for coordination of transition metal ions in the plane. This conformation is particularly interesting because it strongly stabilizes the coordinated Ag(III) and Cu(III) ions. Only one of the two outer N-atoms is protonated in the neutral species, but the species with both protonated or deprotonated pyrrole N-atoms can be easily obtained in solution by addition of HCl or  $NH_3$  vapour (or other bases), respectively [27]. This interesting behaviour allows one to modulate their electronic properties just by controlling the acid-base characteristics of the solution.

Table 1  
Absorption peak wavelengths and corresponding molar absorptivities (as  $\log_{10}$ ) of the *cis*-doubly *N*-confused porphyrins in acetonitrile solution

H <sub>2</sub> N <sub>2</sub> CP	345 (4.5)	427 (4.7)	472 (sh, 4.4)	580 (sh, 3.8)	623 (4.0)	668 (3.9)	722 (sh, 3.5)	
H <sub>4</sub> N <sub>2</sub> CP <sup>2+</sup>	358 (4.6)	464 (4.8)	510 (4.5)	601 (3.8)	690 (3.9)	750 (3.9)		
HN <sub>2</sub> CP <sup>-</sup>	342 (4.4)	402 (4.4)	450 (sh, 4.6)	477 (4.9)	507 (4.4)	~600 (3.9)	655 (3.9)	718 (3.6)
AgHN <sub>2</sub> CP	364 (4.5)	418 (sh, 4.6)	437 (4.7)	475 (4.4)	511 (sh, 4.1)	570 (3.9)	613 (4.2)	665 (3.9)
AgH <sub>2</sub> N <sub>2</sub> CP <sup>+</sup>	370 (4.5)	470 (4.8)	568 (3.9)	610 (4.0)	650 (3.9)	755 (3.2)		
AgN <sub>2</sub> CP <sup>-</sup>	361 (4.3)	423 (4.7)	473 (4.6)	496 (4.6)	552 (4.0)	625 (3.9)	680 (3.5)	
CuHN <sub>2</sub> CP	367 (4.6)	415 (sh, 4.6)	437 (4.8)	475 (4.5)	569 (4.0)	606 (4.3)	670 (3.9)	
CuH <sub>2</sub> N <sub>2</sub> CP <sup>+</sup>	368 (4.5)	466 (4.9)	562 (3.9)	608 (4.1)	644 (3.9)	758 (3.4)		
CuN <sub>2</sub> CP <sup>-</sup>	353 (4.4)	423 (4.8)	469 (4.7)	495 (4.6)	544 (4.1)	595 (4.0)	683 (3.6)	

sh:shoulder.

The free base H<sub>2</sub>N<sub>2</sub>CP in acetonitrile solution exhibits an absorption band profile similar to that found previously in CH<sub>2</sub>Cl<sub>2</sub> [27], as can be seen in Table 1. The small shifts in peak positions were ascribed to solvent effects. It should be noted that the lowest energy absorption band of the neutral and deprotonated species were similar and found around 720 nm, respectively, but was red shifted to 750 nm in the protonated species. This characteristic was confirmed by the emission and excitation spectra shown in Fig. 2, where the first two species exhibit the fluorescence band around 737 nm but is red shifted to 820 nm for the last one. The absorption spectra of the doubly *N*-confused porphyrin species are different from that of porphyrins and *N*-confused tetraphenylporphyrin [28]. The lower symmetry and aromaticity of the *cis*-N<sub>2</sub>CP ring should be responsible for the observed differences, where a reminiscence of a porphyrin spectral profile can be observed particularly for the HN<sub>2</sub>CP<sup>-</sup> species. However, they still exhibit relatively strong absorption and emission bands in the porphyrin spectral region and small Stokes shifts, indicating that the free base H<sub>2</sub>N<sub>2</sub>CP ring is preserving a significant degree of aromaticity and the low energy bands can be assigned to  $\pi$ - $\pi^*$  transitions.

No significant changes in the emission or excitation profiles were observed by varying the excitation wavelength or the monitoring emission wavelength, as can be inferred from the similarity between the absorption and excitation spectra shown in Fig. 2. Analogous behavior was observed for the protonated and deprotonated species. Despite the similarity of the transition energies, the H<sub>2</sub>N<sub>2</sub>CP emission band is much broader and less resolved than that of HN<sub>2</sub>CP<sup>-</sup> species. The luminescence quantum yield of the protonated species ( $0.2 \times 10^{-3}$ ) is more than one order of magnitude smaller than that for the neutral ( $9.1 \times 10^{-3}$ ) and deprotonated ( $6.7 \times 10^{-3}$ ) species, probably due to more efficient thermal decay pathways associated with structural changes. The measured singlet state lifetime of H<sub>2</sub>N<sub>2</sub>CP is 1.0 ns, comparable to that found by Belair [28] for NCP (1.6 ns) and shorter than for TPP (9.2 ns in CHCl<sub>3</sub>). The Stokes shift for the neutral species was only  $151 \text{ cm}^{-1}$ , smaller than for *N*-confused porphyrin ( $371 \text{ cm}^{-1}$ ) and comparable to TPP ( $143 \text{ cm}^{-1}$ ), indicating that the ground state nuclear

coordinates are not very much displaced in relation to the excited state ones. But, it increased to 400 and ca.  $900 \text{ cm}^{-1}$  for the deprotonated and protonated species, respectively, suggesting that they have much distorted excited state conformations.

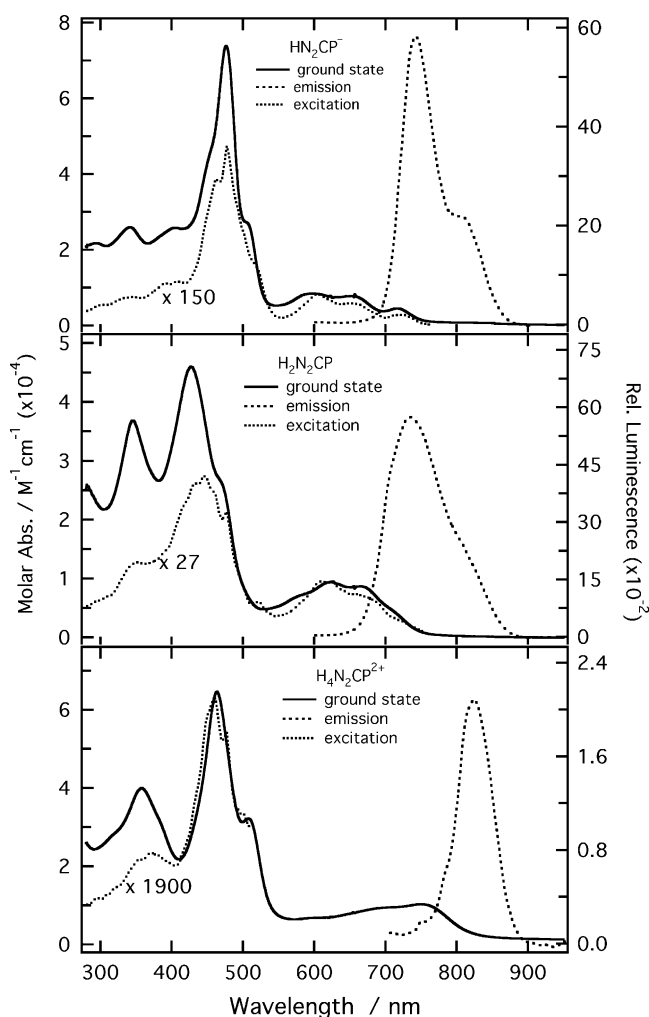


Fig. 2. Absorption (left scale) and excitation-emission (right scale) spectra of HN<sub>2</sub>CP<sup>-</sup>, H<sub>2</sub>N<sub>2</sub>CP and H<sub>4</sub>N<sub>2</sub>CP<sup>2+</sup> species in deaerated acetonitrile solution, at 25 °C.

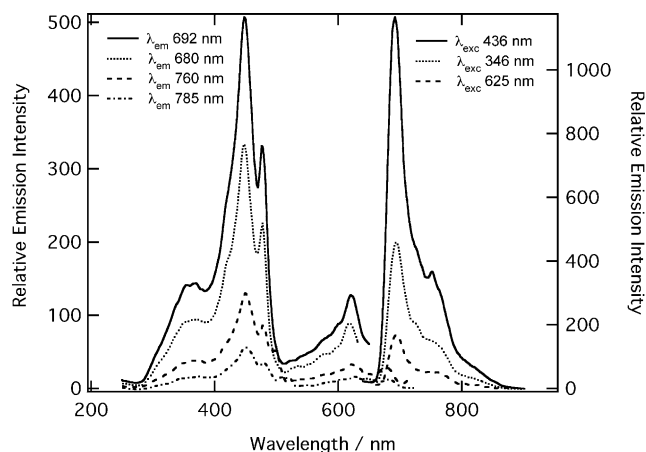


Fig. 3. Excitation (left) and emission (right) spectra of  $\text{H}_2\text{N}_2\text{CP}$  in ethanol glass (77 K) at different excitation or monitoring emission wavelengths, as indicated in the figure.

A significant change in the emission spectrum profile of the neutral species in ethanol glass (Fig. 3) and at room temperature was observed also. The luminescence spectrum profile in ethanol (739 nm and shoulder at  $\sim 817$  nm) is very similar to that in acetonitrile (730 nm and shoulder at  $\sim 813$  nm, Fig. 2), but the bands are slightly red shifted. The spectrum at 77 K exhibits an intense and sharp band at 692 nm and a shoulder at 760 nm, which are about 50 nm blue-shifted in relation to the corresponding spectrum at 298 K, as a consequence of matrix effects.

Generally, the presence of transition metal ions in unusually high oxidation states completely quenches the luminescence of a macrocyclic ligand [30]. Indeed no detectable fluorescence could be observed for the  $\text{Cu}^{\text{III}}\text{HN}_2\text{CP}$  and  $\text{Ag}^{\text{III}}\text{HN}_2\text{CP}$  complexes, as expected for the availability of rapid non-radiative relaxation pathways competing with the radiative decay. The direct thermal relaxation to the ground state is one of the possible pathways, but is competing with the intersystem crossing process to the triplet state, considering that no other unimolecular or bimolecular processes are taking place. In our case, the relaxation rate can be significantly enhanced by an electron transfer mechanism involving the coordinated  $\text{M}(\text{III})$  ion. Nevertheless, the efficiency

of the metal complexes for singlet oxygen generation was found to be much higher than for the free base, as described below. Consequently, the electron transfer mechanism can be ruled out and the metal ion must be enhancing the intersystem crossing quantum yield by increasing its rate, by decreasing the intrinsic thermal decay rate or both.

The triplet state lifetimes were measured by means of the flash-photolysis technique, in absorption mode, and the differential spectra are compared with the electronic spectra in Fig. 4. A strong bleaching of the absorption bands in the 400–500 nm region, consistent with a triplet excited state localized on the macrocyclic ligand [31], can be observed. The lifetimes (Table 2) in the 1.1–1.8  $\mu\text{s}$  range are comparable to those of  $[\text{Ru}(\text{bipy})_3]\text{Cl}_2$  analogues and some porphyrins [32]. The neutral species had the longest triplet state lifetimes and, interestingly, the lifetimes of the metal complexes showed a tendency to be slightly longer than for the free base. This corroborates the assumption that the coordination of  $\text{Ag}(\text{III})$  or  $\text{Cu}(\text{III})$  ions is in fact contributing to slow down the intrinsic thermal decay. It also confirms the previous electrochemistry results [27] showing that those metal ions were stabilized by  $\text{H}_2\text{N}_2\text{CP}$  coordination, losing their typical strong oxidizing character. Presumably, the main thermal relaxation pathways suppressed by coordination of the metal ion are those involving the dipole-dipole coupling of the inner ring hydrogen atoms with the solvent and the ring distortion modes.

### 3.1. Sensitization of singlet oxygen

The oxygen molecule can be found in two singlet excited states that are 0.97 and 1.63 eV above the ground state [33]. This means that the singlet excited state of  $\text{H}_2\text{N}_2\text{CP}$  (1.7 eV, estimated from the absorption and fluorescence spectra) almost perfectly matches the energy requirement to excite the  $\text{O}_2(^3\Sigma_g^-)$  to the  $\text{O}_2(^1\Sigma_g^+)$  state; the most energetic state that quantitatively decays to the lower and more stable  $\text{O}_2(^1\Delta_g)$  state. Generally the singlet excited state is too short lived to be the main sensitizer, so that energy transfer are generally promoted by the less energetic triplet excited state (around 1.1–1.2 eV). This is probably the case

Table 2

Triplet state lifetime ( $\tau_0^T$ ) in  $\text{N}_2$ -saturated solution, bimolecular quenching rate constants ( $k_{\text{photodec}}$ ) and singlet oxygen quantum yields ( $\phi_\Delta$ ) for the doubly *N*-confused porphyrins

	$\tau_0^T$ ( $\mu\text{s}$ )	$k_{\text{photodec}}$ ( $\text{M}^{-1}\text{s}^{-1} \times 10^{-8}$ )	TRIL	$\phi_\Delta$ (532 nm)	TRIL	$\phi_\Delta$ ( $k_d/k_r \times 10^5$ )	480 nm DPBF
$\text{H}_2\text{N}_2\text{CP}$	1.2	9.8		0.19		0.20	(0.98)
$\text{H}_4\text{N}_2\text{CP}^{2+}$	1.4	5.4		0.12		–	
$\text{HN}_2\text{CP}^-$	0.6	7.1		0.13		–	
$\text{AgHN}_2\text{CP}$	1.8	1.9		0.81		0.92	(1.08)
$\text{AgH}_2\text{N}_2\text{CP}^+$	1.1	0.42		0.67		–	
$\text{AgN}_2\text{CP}^-$	1.1	5.6		0.71		–	
$\text{CuHN}_2\text{CP}$	1.4	11.7		0.48		0.66	(1.14)
$\text{CuH}_2\text{N}_2\text{CP}^+$	0.1	1.9		0.22		–	
$\text{CuN}_2\text{CP}^-$	1.2	16.0		0.45		–	

The data obtained by time-resolved infrared luminescence (TRIL) and by quenching with DPBF in acetonitrile solution are listed.

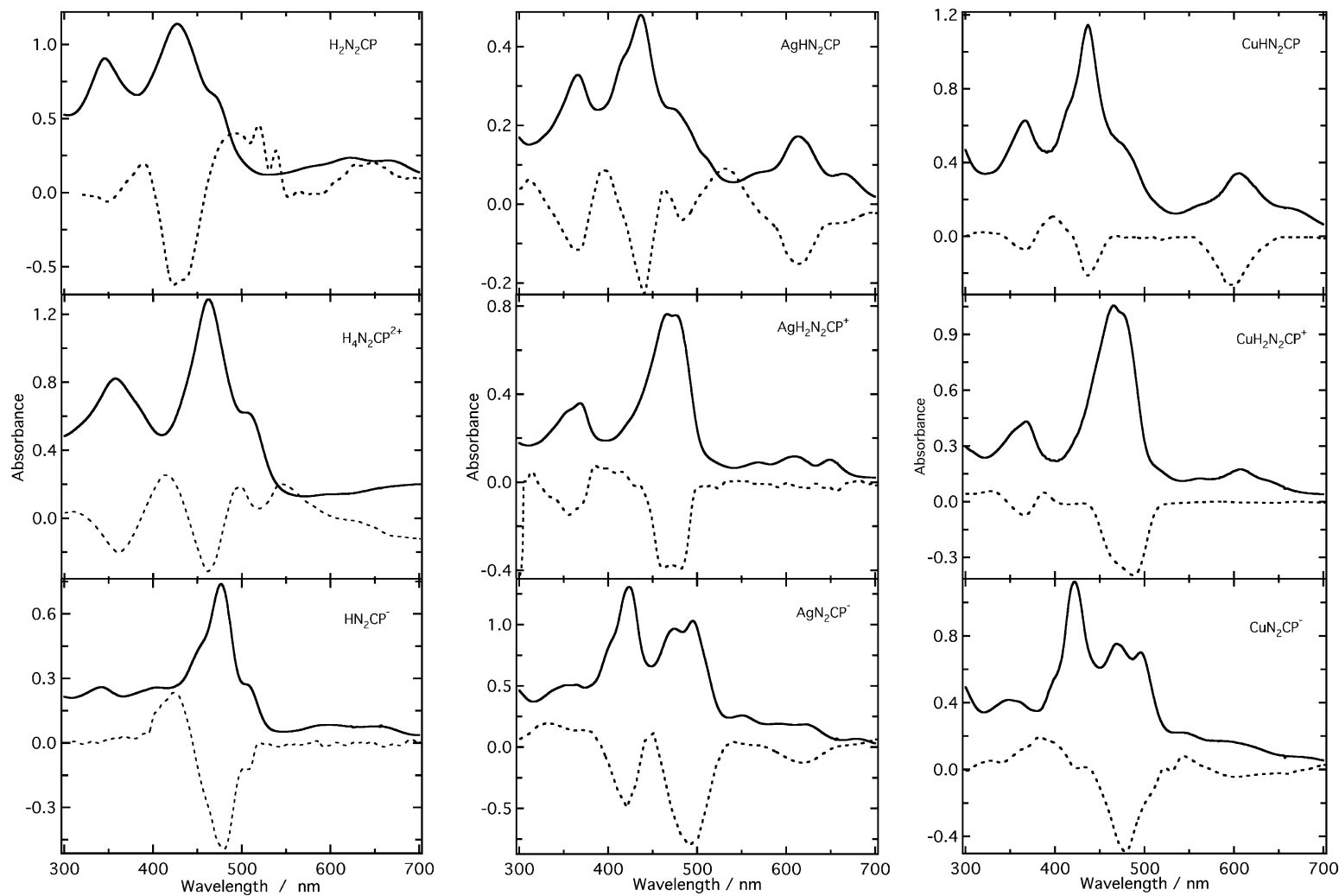


Fig. 4. Absorption spectra (solid line) and differential triplet–triplet transient spectra (dashed line) of free base (left), Ag<sup>III</sup> (center), and Cu<sup>III</sup> (right) in the neutral (top), protonated (middle) and deprotonated (bottom) forms, respectively, in N<sub>2</sub>-saturated solution.

for  $\text{H}_2\text{N}_2\text{CP}$  which should be able to sensitize exclusively the direct formation of  $\text{O}_2(^1\Delta_g)$  because of its somewhat lower energy content in that electronic state. The same reasoning should apply for the Ag(III) and Cu(III) complexes and for the respective deprotonated species since the energies of their lowest absorption band are similar. The protonated species exhibits the lowest energy absorption band at 760 nm, which is shifted up to 90 nm to the red, in comparison with the neutral species.

The singlet oxygen is a very reactive species [34,35], responsible for photodegradation processes that may lead to photocarcinogenesis and photodecomposition like that observed in photobleaching processes. However, this species was shown to efficiently kill tumoral tissues and therapeutic drugs based in its photoinduced generation are receiving regulatory approval in many countries. Consequently, the preparation of new compounds able to efficiently transfer energy to molecular oxygen is of great interest from both, scientific and applied points of view. Accordingly, we measured the singlet oxygen generation quantum yields for doubly *N*-confused porphyrins by monitoring the intensity of  $\text{O}_2(^1\Delta_g)$  phosphorescence at 1270 nm, after a laser shot of 5 ns width. The neutral, protonated, and deprotonated free base  $\text{H}_2\text{N}_2\text{CP}$  species were found to be poor sensitizers, exhibiting quantum yields in the 0.2 range (Table 2). Interestingly, the Ag(III) complex is more efficient ( $\phi_\Delta = 0.81$ ) than the methylene blue used as standard ( $\phi_\Delta = 0.5$ ). In fact, that quantum yield is superior to that measured for TPP in toluene ( $\phi_\Delta = 0.73$ ) and monoacidic benzoporphyrin ( $\phi_\Delta = 0.76$ ). This is the active species of Visudyne<sup>®</sup>, the phototherapeutic drug recently approved by FDA for treatment of macular neovascularization [36–38]. The Cu(III) complex exhibited intermediary quantum yields. Finally, it is evident from Table 2 that the activity follows the tendency neutral > deprotonated > protonated species.

In order to confirm the results obtained by  $\text{O}_2(^1\Delta_g)$  phosphorescence laser flash photolysis, the quantum yields for the neutral species were evaluated employing DPBF (1,3-diphenylisobenzofuran), as described by Spiller et al [39]. This species exhibits a strong absorption band at 411 nm that disappears when oxidized by singlet oxygen (the reaction product does not have bands in the 250–1000 nm range). Photodecomposition was minimized in this case because a light source of lower intensity (Oriol Spectral Luminator) was employed in the experiments. The quantum yield  $\phi_\Delta$  was calculated [39,40] using the Eq. (1).

$$-\frac{d[\text{DPBF}]}{dt} = -\frac{dA}{dt} \frac{1}{\varepsilon_{\text{DPBF}} l} = I_a \phi_\Delta \frac{k_r [\text{DPBF}]}{k_r [\text{DPBF}] + k_d} \quad (1)$$

where  $A$  is the absorbance,  $\varepsilon_{\text{DPBF}}$  ( $2.2\text{--}2.3 \times 10^4 \text{ M}^{-1} \text{ cm}^{-1}$ ) [39] the molar absorption of DPBF at 411 nm,  $I_a$  the total absorbed photon flux per unit volume and unit time,  $l$  the optic path length,  $k_d$  the  $^1\text{O}_2$  decay rate constant, and  $k_r$  is the  $^1\text{O}_2$  quenching rate constants by DPBF. The  $I_a \phi_\Delta$  and

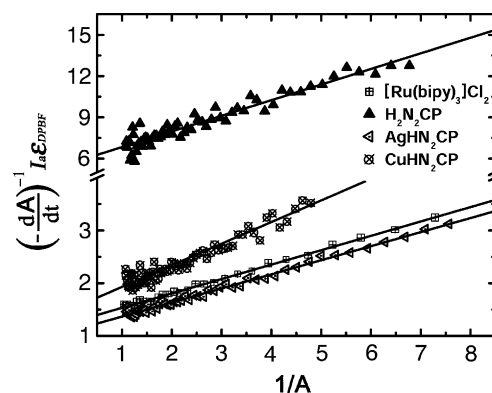


Fig. 5. Plots of  $I_a \varepsilon_{\text{DPBF}} (-dA/dt)^{-1}$  vs.  $1/A$ , the reciprocal of the DPBF absorption at 411 nm according to Eq. (2), using  $[\text{Ru}(\text{bipy})_3]\text{Cl}_2$  (30  $\mu\text{M}$ ),  $\text{H}_2\text{N}_2\text{CP}$  (9  $\mu\text{M}$ ),  $\text{AgHN}_2\text{CP}$  (8  $\mu\text{M}$ ) or  $\text{CuHN}_2\text{CP}$  (5  $\mu\text{M}$ ) as singlet oxygen sensitizer ( $\lambda_{\text{exc}} = 480 \text{ nm}$ ), in air saturated acetonitrile solutions.  $[\text{DPBF}] = 45 \mu\text{M}$ ,  $I_{480} = 1.15 \times 10^{-7} \text{ M s}^{-1}$ .

$k_r/k_d$  can be obtained from the intercept and slope/intercept ratio of  $(dA/dt)^{-1}$  versus  $A^{-1}$  plots according to Eq. (2).

$$-\left[\frac{dA}{dt}\right]^{-1} = \frac{1}{I_a \phi_\Delta \varepsilon_{\text{DPBF}} l} = \frac{k_d}{k_r I_a \phi_\Delta} \frac{1}{A} \quad (2)$$

However, to calculate  $\phi_\Delta$  it is necessary to determine  $I_a$ , a parameter that depends on the experimental arrangement. It was evaluated as being  $1.15 \times 10^{-7} \text{ M s}^{-1}$  by using  $[\text{Ru}(\text{bipy})_3]\text{Cl}_2$  ( $\phi_\Delta = 0.8$  at 480 nm) as standard. The plots of  $I_a \varepsilon_{\text{DPBF}} (-dA/dt)^{-1}$  versus  $1/A$  for the standard and the doubly *N*-confused porphyrins are shown in Fig. 5. The quantum yields obtained by this method were more reproducible than those measured by TRIL and are listed in Table 2. The value of  $k_d/k_r$ , where  $k_d = 1.3 \times 10^4 \text{ s}^{-1}$  is the lifetime of singlet oxygen in acetonitrile [33] and  $k_r$  the reaction rate constant with DPBF, are shown in parenthesis. That ratio is not varying very much (average value =  $1.1 \times 10^{-5} \text{ M}$ ), as expected for results obtained in a same solvent. Accordingly,  $k_r$  was estimated as being  $1.2 \times 10^9 \text{ M}^{-1} \text{ s}^{-1}$ , close to diffusion controlled reaction rates and in the same order of magnitude of the values found in DMF and methanol [39]. That is about one order of magnitude lower than those found for charge transfer quenching of strong electron donor amines and some aromatic compounds in cyclohexane and benzene [41].

The quantum yields obtained by both methods were identical for the free base, within experimental error, but were significantly higher for Ag(III) and Cu(III) complexes (14 and 27%, respectively), as shown in Table 2. Similar results were obtained by using methylene blue as standard and excitation wavelength of 600 nm. Such relatively large differences between the chemical and photophysical methods has been previously reported [39,42] and assigned to the use of different wavelengths for the excitation of the standard and the compounds in the experiments. This does not apply in our case and probably is reflecting the contribution of photodecomposition processes in the TRIL method. This is particularly important in the case of the Cu(III) complex, that

was shown to be the most reactive species and a relatively good sensitizer for singlet oxygen generation, as shown below.

### 3.2. Photodecomposition of *cis*-doubly *N*-confused porphyrins

An inspection of the  $O_2(^1\Delta_g)$  phosphorescence decay curves showed that the slope of the  $\log_{10}$  plot varies as a function of the sensitizer concentration (Fig. 6). This is consistent with the occurrence of a second order reaction where the photogenerated  $^1O_2$  is being quenched by the sensitizer itself. In order to elucidate the nature of the quenching process, a careful study was carried out changing the experimental conditions. We found out that *cis*-doubly *N*-confused porphyrins are stable in argon or nitrogen gas purged acetonitrile solution, when irradiated with a filtered 150 W Xenon lamp to remove the infrared and the high energy fraction of the UV radiation. A quite fast photobleaching was observed though in oxygenated solutions. In fact, we found out that even a very small amount of oxygen, which may be diffusing through the septum, was enough to promote a slow but steady decay of the absorbance as a function of the irradiation time.

The irradiation of the samples leads to the disappearance of the doubly *N*-confused porphyrin bands in the 350–500 nm and 600–750 nm range within 45 min and to the rise of two new bands at 320–540 nm, clearly indicating the occurrence of a photoreaction process. The absorption spectra of the free base, Cu(III) and Ag(III) complexes after irradiation were similar, suggesting that the photoproducts may be the same (Fig. 7). The higher reactivity of the copper derivative is evidenced in the comparative kinetic curves (Fig. 8), where it is shown to be completely decomposed after 10 min while the free base and silver derivatives required up to 45 min, in the same experimental conditions. The decay curves were tentatively fitted using a single

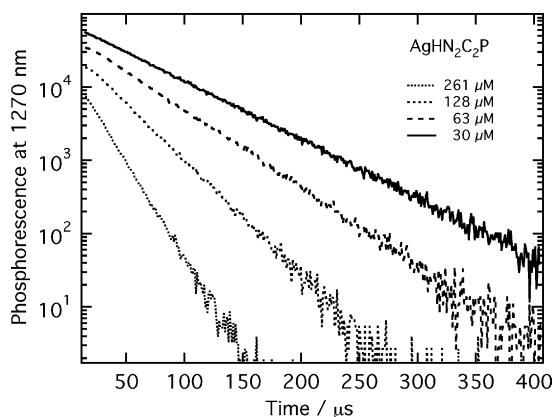


Fig. 6. Decay of the  $^1O_2$  phosphorescence emission at 1270 nm as a function of the time and concentration of  $AgHN_2CP$ , in air saturated solution ( $[O_2] = 1.9 \text{ mM}$ ). The curves were normalized by the concentration of the sensitizer and plotted in  $\log_{10}$  scale.

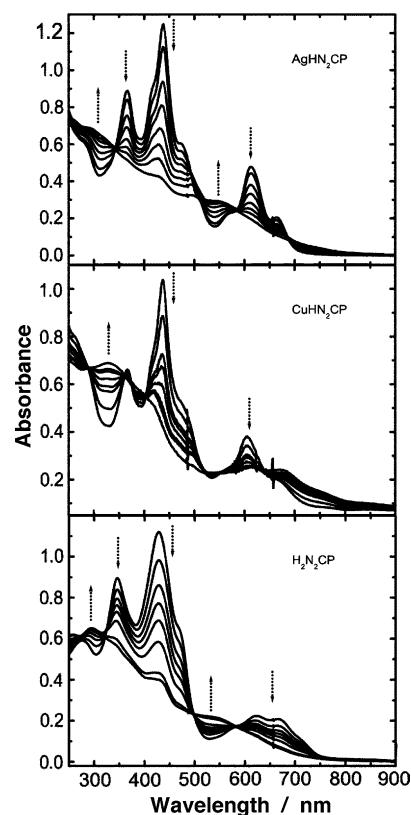


Fig. 7. Decay (photobleaching) of the UV-Vis absorption bands as a function of the time for  $CuHN_2CP$  (10 min),  $AgHN_2CP$  (45 min), and  $H_2N_2CP$  (45 min) in  $O_2$  saturated acetonitrile solutions.

exponential, which was satisfactory for the metal complexes. A double exponential was more suitable for the free base species but the contribution of the slower component was estimated to be less than 10%. The calculated pseudo-first order rate constants are 0.10,  $\sim 2 \times 10^{-3}$ , and  $1.7 \times 10^{-3} \text{ s}^{-1}$ , respectively, for the  $CuHN_2CP$ ,  $H_2N_2CP$  and  $AgHN_2CP$  derivatives in  $O_2$  saturated acetonitrile

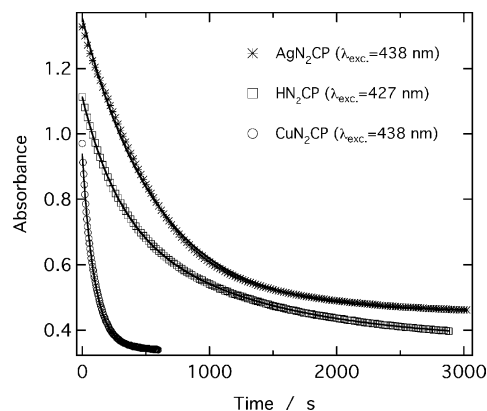


Fig. 8. Absorbance decay curves as a function of the time for  $AgHN_2CP$ ,  $CuHN_2CP$  and  $H_2N_2CP$ , in  $O_2$ -saturated acetonitrile solution, at  $\lambda_{exc} = 438$  and 427 nm. The  $AgN_2CP$  curve was offset 0.08 a.u. for better visualization. The solid lines are the exponential or double exponential (free base) curve fittings.

solution. As one can notice by these results, the Cu(III) complex is about 60 times more reactive than the free base or the Ag(III) complex, but the reasons could not be clarified yet [43].

The actual second order rate constants can be evaluated by means of the Stern–Volmer plots of the  $O_2(^1\Delta_g)$  phosphorescence emission decay curves at 1270 nm as a function of the sensitizer concentration and the  $k_{\text{photodec}}$  values are listed in Table 2. The Cu(III) complex is the most reactive species, followed by the free base and the Ag(III) complex, in agreement with the photostability experiment results. In addition, the local concentration of singlet oxygen can be estimated as been about  $10^{-10}$ – $10^{-11}$  M, if one considers that the pseudo-first order rate constants obtained in those experiments can be expressed as  $k_{\text{photodec}}[O_2(^1\Delta_g)]$ . This is significantly smaller than  $[O_2] = 1.9$  mM (in air saturated acetonitrile solution) indicating that only a very small fraction of the available oxygen molecules is being activated by energy transfer, as expected.

#### 4. Conclusions

The photophysical properties of the free base, Ag(III) and Cu(III) complexes of *cis*-doubly *N*-confused porphyrin have been examined by means of electronic and time-resolved spectroscopy. The slight tendency of increase of the triplet lifetimes ( $\sim 1$   $\mu$ s) associated with the enhanced singlet oxygen quantum yields found for the complexes (up to 0.92) are strong evidence that the vibrational relaxation was significantly suppressed while the intersystem crossing quantum yield was enhanced by coordination of the M(III) ion. All species are relatively stable in oxygen free solutions but are more or less rapidly bleached by reaction with singlet oxygen ( $k_r \sim 1 \times 10^9$  M<sup>-1</sup> s<sup>-1</sup>). This may be one of the probable factors responsible for the higher quantum yields found by using the chemical method instead of the time resolved infrared phosphorescence method. The Cu(III) complex is much more reactive than the free base and Ag(III) species, but the reasons deserve further studies. In summary, our results showed that Ag(III) complex is an excellent singlet oxygen generator and may be useful as photosensitizer for applications that do not require extended stability and high concentrations. This may be the case of PDT [44] in which a certain degree of decomposition is beneficial, because it accelerates the elimination process, minimizing long term photosensibility, as for the case of Visudyne®.

#### Acknowledgements

The authors thank Fundação de Amparo à Pesquisa do Estado de São Paulo, Conselho Nacional de Desenvolvimento Científico e Tecnológico and RENAMI, for the financial support.

#### References

- [1] H. Furuta, T. Asano, T. Ogawa, J. Am. Chem. Soc. 116 (1994) 767–768.
- [2] P.J. Chmielewski, L. Latos-Grazynski, K. Rachlewicz, T. Glowiak, Angew. Chem. Int. Edit. Engl. 33 (1994) 779–781.
- [3] L. Latos-Grazynski, in: K.M. Kadish, K.M. Smith, R. Guilard (Eds.), The Porphyrin Handbook, vol. 2, Academic Press Inc., San Diego, 2000.
- [4] H. Furuta, H. Maeda, A. Osuka, Chem. Commun. (2002) 1795–1804.
- [5] P.J. Chmielewski, L. Latos-Grazynski, T. Glowiak, J. Am. Chem. Soc. 118 (1996) 5690–5701.
- [6] P.J. Chmielewski, L. Latos-Grazynski, Inorg. Chem. 36 (1997) 840–845.
- [7] P.J. Chmielewski, L. Latos-Grazynski, Inorg. Chem. 39 (2000) 5639–5647.
- [8] H. Furuta, N. Kubo, H. Maeda, T. Ishizuka, A. Osuka, H. Nanami, T. Ogawa, Inorg. Chem. 39 (2000) 5424–5425.
- [9] H. Furuta, K. Youfu, H. Maeda, A. Osuka, Angew. Chem. Int. Edit. 42 (2003) 2186–2188.
- [10] P.J. Chmielewski, L. Latos-Grazynski, I. Schmidt, Inorg. Chem. 39 (2000) 5475–5482.
- [11] H. Maeda, A. Osuka, Y. Ishikawa, I. Aritome, Y. Hisaeda, H. Furuta, Org. Lett. 5 (2003) 1293–1296.
- [12] H. Furuta, T. Ogawa, Y. Uwatoko, K. Araki, Inorg. Chem. 38 (1999) 2676–2682.
- [13] H. Maeda, Y. Ishikawa, T. Matsuda, A. Osuka, H. Furuta, J. Am. Chem. Soc. 125 (2003) 11822–11823.
- [14] H. Furuta, T. Ishizuka, A. Osuka, T. Ogawa, J. Am. Chem. Soc. 121 (1999) 2945–2946.
- [15] H. Furuta, T. Ishizuka, A. Osuka, T. Ogawa, J. Am. Chem. Soc. 122 (2000) 5748–5757.
- [16] H. Furuta, T. Ishizuka, A. Osuka, H. Dejima, H. Nakagawa, Y. Ishikawa, J. Am. Chem. Soc. 123 (2001) 6207–6208.
- [17] H. Furuta, T. Ishizuka, A. Osuka, Y. Uwatoko, Y. Ishikawa, Angew. Chem. Int. Ed. 40 (2001) 2323–2325.
- [18] A. Srinivasan, H. Furuta, A. Osuka, Chem. Commun. (2001) 1666–1667.
- [19] H. Furuta, T. Ishizuka, A. Osuka, J. Am. Chem. Soc. 124 (2002) 5622–5623.
- [20] J.C. Liu, T. Ishizuka, A. Osuka, H. Furuta, Chem. Commun. (2003) 1908–1909.
- [21] H. Furuta, H. Maeda, A. Osuka, J. Am. Chem. Soc. 122 (2000) 803–807.
- [22] H. Furuta, H. Maeda, A. Osuka, M. Yasutake, T. Shinmyozu, Y. Ishikawa, Chem. Commun. (2000) 1143–1144.
- [23] H. Maeda, A. Osuka, H. Furuta, Supramol. Chem. 15 (2003) 447–450.
- [24] H. Furuta, H. Maeda, A. Osuka, J. Org. Chem. 65 (2000) 4222–4226.
- [25] H. Furuta, H. Maeda, A. Osuka, J. Org. Chem. 66 (2001) 8563–8572.
- [26] H. Maeda, A. Osuka, H. Furuta, J. Am. Chem. Soc. 125 (2003) 15690–15691.
- [27] K. Araki, H. Winnischofer, H.E. Toma, H. Maeda, A. Osuka, H. Furuta, Inorg. Chem. 40 (2001) 2020–2025.
- [28] J.P. Belair, C.J. Ziegler, C.S. Rajesh, D.A. Modarelli, J. Phys. Chem. A 106 (2002) 6445–6451.
- [29] K. Araki, F.M. Engelmann, I. Mayer, H.E. Toma, M.S. Baptista, H. Maeda, A. Osuka, H. Furuta, Chem. Lett. 32 (2003) 244–245.
- [30] L. Flamigni, F. Barigelletti, N. Armaroli, J.P. Collin, J.P. Sauvage, J.A.G. Williams, Chem. Eur. J. 4 (1998) 1744–1754.
- [31] K. Araki, P. Losco, F.M. Engelmann, H. Winnischofer, H.E. Toma, J. Photochem. Photobiol. A. 142 (2001) 25–30.
- [32] K. Kalyanasundaram, Photochemistry of Polypyridines and Porphyrin Complexes, Academic Press, London, 1992.
- [33] C. Schweitzer, R. Schmidt, Chem. Rev. 103 (2003) 1685–1757.
- [34] R.W. Redmond, J.N. Gamlin, Photochem. Photobiol. 70 (1999) 391–475.



- [35] P. Dimascio, E.J.H. Bechara, M.H.G. Medeiros, K. Briviba, H. Sies, *FEBS Lett.* 355 (1994) 287–289.
- [36] J.W. Miller, U. Schmidt-Erfurth, M. Sickenberg, C.J. Pournaras, H. Laqua, I. Barbazetto, L. Zografos, B. Piguët, G. Donati, A.M. Lane, R. Birngruber, H. Van Den Berg, H.A. Strong, U. Manjuri, T. Gray, M. Fsadni, N.M. Bressler, E.S. Gragoudas, *Arch. Ophthalmol.* 117 (1999) 1161–1173.
- [37] U. Schmidterfurth, T.J. Flotte, E.S. Gragoudas, K. Schomacker, R. Birngruber, T. Hasan, *Exp. Eye Res.* 62 (1996) 1–10.
- [38] U. Schmidt-Erfurth, J. Miller, M. Sickenberg, A. Bunse, H. Laqua, E. Gragoudas, L. Zografos, R. Birngruber, H. Van Den Bergh, A. Strong, U. Manjuri, M. Fsadni, A.M. Lane, B. Piguët, N.M. Bressler, *Graefes Arch. Clin. Exp. Ophthalmol.* 236 (1998) 365–374.
- [39] W. Spiller, H. Kliesch, D. Wöhrle, S. Hackbarth, B. Roder, G. Schnurpfeil, *J. Porphyrins Phthalocyanines* 2 (1998) 145–158.
- [40] J.L. Bourdelande, M. Karzazi, L.E. Dicalio, M.I. Litter, G.M. Tura, E. Sanroman, V. Vinent, *J. Photochem. Photobiol. A* 108 (1997) 273–282.
- [41] A.P. Darmanyan, W. Lee, W.S. Jenks, *J. Phys. Chem. A* 103 (1999) 2705–2711.
- [42] G. Valduga, S. Nonell, E. Reddi, G. Jori, S.E. Braslavsky, *Photochem. Photobiol.* 48 (1988) 1–5.
- [43] H. Furuta, H. Maeda, A. Osuka, *Org. Lett.* 4 (2002) 181–184.
- [44] E.D. Sternberg, D. Dolphin, C. Bruckner, *Tetrahedron* 54 (1998) 4151–4202.